Extracted Strand Magnetizations of an HQ Type Nb_3Sn Rutherford Cable and Estimation of Transport Corrections at Operating and Injection Fields

Edward W. Collings, Mike A. Susner, Mike D. Sumption, and Daniel R. Dietderich

***Abstract*—One of the goals of the Large Hadron Collider Accelerator Research Program (LARP) is to demonstrate the feasibility of Nb_3Sn technology for a proposed luminosity upgrade based on large aperture high gradient quadrupole (HQ) magnets. For such magnets field quality at the bore is a critical requirement for which reason the parasitic magnetization of the windings must be reduced to manageable limits. In other words it is necessary to minimize (i) the static intrastrand persistent-current magnetization of the cable and (ii) the cable's coupling magnetization caused by coupling currents passing through interstrand contact resistance during field ramping. This report focuses on persistent-current magnetization as measured by vibrating-sample magnetometry on pieces of strand removed from a section of heat treated HQ cable.**

***Index Terms*— Large Hadron Collider, high gradient quadrupole, Nb_3Sn strand, persistent current magnetization, cable magnetization, bore field quality**

I. Introduction

After its initial start-up in September 2008 the Large Hadron Collider (LHC) has been operating regularly since March 2010, collecting data that during July 2012 to March 2013 offered evidence for the discovery of the elusive Higgs particle [1], even while operating at a collision energy of 4 TeV/beam, much less than the design value. After a planned shut-down of almost two years for maintenance and infrastructure improvement (LS1, 2013-14) [2] the LHC will commence operating at its design energy of 7 TeV/beam and continue to push the frontiers of high energy particle physics. The LHC's superconducting magnets are all wound with NbTi Rutherford cables. Contributing to the LHC's success are what might be termed the qualities of the dipole and quadrupole fields, great care having been taken to control parasitic magnetization in the magnet windings and other magnetic effects. The magnetic properties and field qualities of the LHC's present NbTi magnets provide bench-marks against which those of any future magnets can be compared.

Manuscript received July 15, 2013. Funding was provided by the U.S. Dept. of Energy, Office of High Energy Physics, under Grants No. DE-FG02-95ER40900 (OSU) and DE-AC02-05CH11231 (LBNL).

E.W. Collings, M.D. Sumption, and M.A. Susner are with the Center for Superconducting and Magnetic Materials (CSMM), Dept. of Materials Science and Engineering, The Ohio State University, USA.

D .R. Dietderich is with the Superconducting Magnet Group, Lawrence Berkeley National Laboratory (LBNL), University of California, USA.

Looking ahead, a series of upgrades to the accelerator are planned, many of them requiring cables/magnets wound with superconductors with higher performances than NbTi -- Nb_3Sn, HTS, and combinations of them [3]. (1) Beam collimation is to be improved by the installation of additional collimators in the dispersion-suppressor (DS) segments of the ring. To make room for these with minimal disruption to the existing line it is proposed to replace pairs of 8.33 T, 15 m, NbTi dipoles with pairs of 11 T, 11 m, Nb_3Sn dipoles [4]. The new magnets will need to be fully compatible (dimensions, field harmonic content, etc) with the NbTi magnets they are to replace [3][4]. In particular, when exchanging NbTi for Nb_3Sn, particular attention will need to be given to differences in parasitic magnetization. Some strand and cable specifications for the 11 T DS dipole are listed in Table I. (2) The LHC's "High Lumi" luminosity upgrade calls for the installation by 2022-2023 of sixteen low-β quadrupole magnets with aperture 120-150 mm, length 8-10 m, peak field 13 T (conductor field 15 T), and a yet-to-be-determined gradient higher than 120 T/m [3][5].

II. Bench-Mark Values For Parasitic Magnetizations Of Rutherford Cables Based On The NbTi LHC-Inner Cable

A. Coupling Magnetization

An estimate of the LHC's inner-cable coupling magnetization at the specified charging rate of 6.5 mT/s can be made by inserting cable parameters into Equation (1) based on an expression due to Sytnikov et al [6] for coupling loss, Q_{coup}, (= $4M_{coup}B_m$,) in a Rutherford cable due to a time-varying field of amplitude B_m directed normal to the cable's flat face (in A/m or J/m^{3}T)

$$M_{coup} = \left(\frac{1}{3}\right)\left(\frac{w}{t}\right)L_p\left(\frac{N^2}{20}\right)\left[\frac{1}{R_c}+\frac{20}{N^3R_a}\right]\left(\frac{dB}{dt}\right) \qquad (1)$$

For the LHC-inner cable the width/thickness ratio (w/t) is 7.94, the lay length (half twist pitch, L_p) is 55 mm, and the strand count is 28. Then based on published recommendations for interstrand contact resistances (ICR) we take 15 μΩ for the crossover resistance (R_c) [7] and 0.2 μΩ for the adjacent-strand resistance (R_a) [8] and find $M_{coup,LHC}$ = 2.64 kA/m.

B. Persistent-Current Magnetization

An increasing field applied to a superconducting strand is shielded by a so-called persistent current equivalent to a Bean-type magnetization, M_{sh} (one half of the full height of a magnetization loop). This leads to a ramp-rate-independent cable magnetization given by $M_{sh} = (2/3\pi)\lambda_s\lambda_c J_c d$ in which λ_s and λ_c are the strand- and cable fill factors, respectively, J_c is the critical current density, and d is the strand's effective filament diameter. For the cable magnetization at the LHC injection field of 0.54 T we combine a J_c (1.9 K, 0.54 T) of 20.4 kA/mm^2 (based on Boutboul et al's measurements of an LHC-insertion-quadrupole strand [9]) with a $d_{LHC\text{-}inner}$ of 7 μm and λ_s and λ_c values of 0.377 and 0.9, respectively, to obtain $M_{sh,inj,LHC}$ = 10.3 kA/m only 4 times larger than the coupling magnetization. Then after extrapolating J_c (after [10]) to the operating field of 8.33 T whereat it becomes 10.0 kA/mm^2, we find $M_{sh,op,LHC}$ = 5.1 kA/m.

Judging by its performance it is clear that the magnetic properties of the LHC's cables have been successfully managed. Thus the values $M_{coup,LHC}$ = 2.64 kA/m and $M_{sh,inj,LHC}$ = 10.3 kA/m, may be regarded as bench-marks against which the corresponding properties of Nb_3Sn cables can be compared.

III. Coupling In Typical Nb_3Sn Cables

Previous publications by this group (e.g, [11-17]) have discussed coupling loss/magnetizations in various Nb_3Sn Rutherford cables that were wound at both the Lawrence Berkeley National Laboratory (LBNL) and Fermi National Accelerator Laboratory (FNAL). As indicated in Equation (1) the ramp-rate dependence of M_{coup} is a function of the cable parameters including an "effective contact resistance", R_{eff}, defined as $[1/R_c + 20/N^3R_a]^{-1}$ [11]. For a Rutherford cable R_{eff} is best obtained from the reciprocal slope of an AC loss (Q) versus applied field ramp-rate (dB/dt) or frequency (f) measurement – either calorimetric [11] magnetic [12]. Since M_{coup} α $1/R_{eff}$, M_{coup} can be confined within an acceptable range of values by ensuring that R_{eff} itself is suitably constrained.

Referring again to the LHC reference ICR values we note that at R_a = 0.2 μΩ its contribution to R_{eff} is $N^3R_a/20$ = 220 μΩ. Such a value ensures current sharing while at the same time its contribution to coupling magnetization is negligible. By the same token, for the LHC cable $R_{eff} \approx R_c$, low enough to contribute to current sharing and high enough to constrain coupling magnetization.

In the standard wind-and-react procedure for magnet fabrication, during which the cable is subjected to uniaxial pressure of several tens of MPa while undergoing prolonged heat treatment including a final 48h/650°C, a very low R_c is produced as the strands become sintered together at their crossover points of contact. Measurements of Nb_3Sn cables over the years have revealed R_c values of 0.09 μΩ, 0.14 μΩ [13], 0.15 μΩ, 0.16 μΩ [14][15], 0.21μΩ [13], 0.24 μΩ [16], 0.3-0.36 μΩ [14][15], and 0.4 μΩ [17]. Assuming an average of 0.23 μΩ a Nb_3Sn cable otherwise conforming to LHC specifications would exhibit a coupling magnetization of 161 kA/m which is 60 times larger than $M_{coup,LHC}$.

As future magnets may require new cables with higher strand counts the R_c criterion will need to be revised. For example an increase of N to 40 (e.g. the DS dipole, Table I) other parameters remaining the same, would require an increase of R_c (or R_{eff}) to 30 ± 10 μΩ. The best way to achieve the desire ICR is to insert an insulating core between the cable's "upper" and "lower" layers. The insertion of the core drives up R_c while leaving R_a unchanged thus preserving the cable's current sharing capacity. Over the years cables with cores of various materials have been tested: bimetallic stainless steel and copper [16], MgO tape [18], E-glass and S-glass ribbon [18][19], and thin stainless steel strip. Using stainless steel cores values of R_{eff} obtained have varied from 0.8 μΩ [19] to 246 μΩ [20] depending on the core's width and placement within the cable. By adjusting these key variables it is in principle possible to tune R_{eff} so as to achieve an acceptable value (or range of values) of M_{coup}.

In support of the LHC's luminosity upgrade the US Accelerator Research Program (LARP) has been developing a series of Nb_3Sn-wound test quadrupoles designated TQ, LQ, and finally HQ, the high gradient quadruple for the High Lumi upgrade [21]. As a contribution to this development program the present group has studied the properties of TQ-class 27-strand Rutherford cables both with and without a stainless steel (SS) core [20]; and as a further contribution we are now directing our attention to the magnetic properties of strand and cable for the quadrupole designated HQ.

IV. Experimental

A. Sample Materials

Wound at LBNL and supplied for measurement to the Ohio State University's Center for Superconducting and Magnetic Materials (OSU-CSMM) were several meters of SS-cored cable of the type specified for HQ. The strand and cable details are listed in Table I, additional measurement and analysis of these and similar cables and strands are given by Godeke [22]. Segments of this cable each about 19 inches long were enclosed in S-glass braid in readiness for assembly into six-high cable packs. Mounted in a special SS fixture they were uniaxially compressed to 20.0 MPa prior to reaction heat treatment (RHT) at Brookhaven National Laboratory (BNL) of 72h/210°C + 48h/400°C + 48h/650°C. The objectives of the present study were the magnetically derived properties of a sample of strand extracted from one of the cable segments, the cables themselves being set aside for possible AC loss measurement, cf. [11][12].

B. Measurements

Vibrating sample magnetometer (VSM) measurements were made on extracted-strand samples using a Quantum Design Model 6000 "physical property measurement system" (PPMS) of fully penetrated M-B loops at 1.9 K to ± 14 T, Fig. 1. Calibrated back-scattered scanning electron microscopy (BS/SEM) performed on polished samples of HQ strand, Fig.

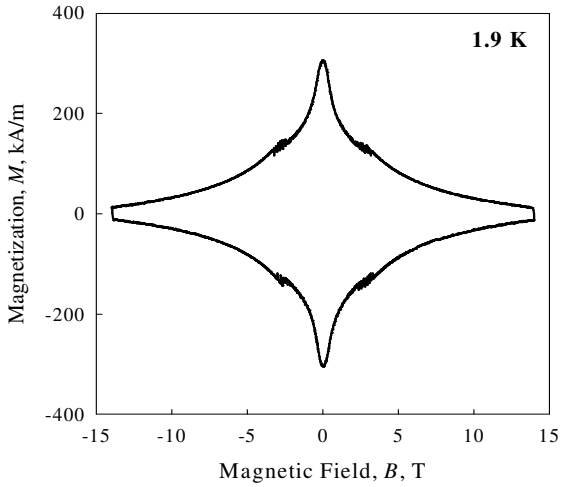

Fig. 1. PPMS-measured *M-B* loop at 1.9 K to ± 14 T.

TABLE I. STRAND AND CABLE DETAILS†

(a) Strand Details	**DS dipole**	**HQ Quadrupole**
OST-RRP Billet ID No.s	--	13091, 13658, 13659
No. of strands per billet, resp.	--	13, 15, 7 (= 35)
Strand type (element #)	108/127	108/127
Filament gggcount††	--	108
Strand diam., mm	0.7	0.778
Av. filament OD, d_o, µm	--	51.5*
Prior internal-Sn diam., d_i, µm	--	28.8*
Effective fil. diam., d_{eff}, µm	--	61.3**
Non-Cu content, %	47.6	44.9
Strand anneal	--	4h/185-190°C
* Measured at OSU by SEM after cable RHT		
** Calculated using $d_{eff} = d_0[(1-R^3)/(1-R^2)]$ with $R = d_i/d_0$ [22]		
(b) Cable Details		
Cable name	--	HQ1021ZB (LBNL)
Cable maker	**FNAL**	**LBNL**
OSU cable name	--	HQ2
Strand count	40	35
Pitch, 2*Lp*, mm	--	95
Width, *w*, mm	14.70	14.77
Av. thick, *t*, mm	1.269	1.375
Keystone angle, deg	0.79	0.722
Average pack's factor, %	--	85.53
Core material	--	AISI 316L
Core width, mm	--	8
Heat treatment (RHT), **BNL**	--	72h/210°C + 48h/400°C + 48h/650°C

† supplied by LBNL (2012), †† Filament (Subelement) count, see Fig 2

2, enabled an average "effective filament diameter" d_{eff} to be derived. As indicated in Table I, d_{eff} is larger than the geometrical outside diameter of the filament (subelement) due to the presence of the non-superconducting central hole, the space occupied by the prior Sn source [23]. Measurements averaged over the entire strand yielded d_{eff} = 61.3 µm.

V. Results And Discussion

A. Critical Current Density and Persistent-Current Magnetization

The magnetically determined critical current densities as function of applied field to 14 T, $J_{c,non\text{-}Cu}(B)$, Fig. 3, were

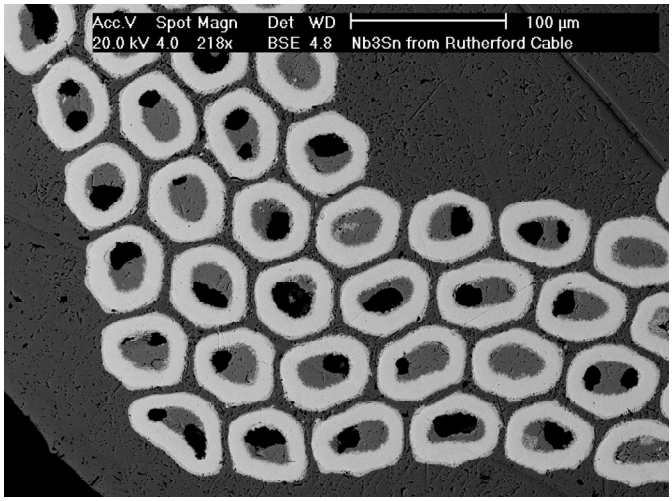

Fig. 2. Segment of OST's RRP 108 filament (subelement) type 108/127 strand viewed by back-scattered SEM -- Philips/FEI Sirion FEG source.

determined from the full height of the *M-B* loop, ΔM, using the "semi-Bean" relationship $J_{c,non\text{-}Cu} = (3\pi/4)\Delta M\lambda d_{eff}$ in which λ represents the superconducting fill factor (non-Cu area/strand area). The resulting $J_{c,non\text{-}Cu}$ and B values were then assembled in the form of a Kramer plot ($J_c^{0.5}B^{0.25}$ versus B, Fig. 4) whose linearity: (i) indicates that the Nb_3Sn layer is grain-boundary pinned such that $J_c(B)$ follows closely a Kramer-Dew-Hughes (KDH) expression for isothermal field dependence, $b^{-1/2}(1-b)^2$, in which $b = B/B_{c2}$ [24] and (ii) enables an upper critical field ($B_{c2,1.9K}$ = 23.01 T) to be obtained by extrapolation. The conformity of $J_c(B)$ to the normal-grain-boundary-pinning model is further illustrated in Fig.5 in which the experimental bulk pinning force density, F_pB, is seen to closely fit the KDH relationship $J_c.B = F_p \propto b^{1/2}(1-b)^2$, enabling the magnetically determined $J_{c,non\text{-}Cu}(B)$ to be extrapolated from 14 T out to higher fields, e.g. 15, 16, and 16.5 T.

Shielding (field-increasing) persistent current magnetizations, $M_{sh,1.9K}$, were extracted from the shielding branch of the *M-B* loop, Fig. 1, and extrapolated from 12 T (measured) to 16 T using the above KDH proportionality, B_{c2} having been obtained by Kramer extrapolation.

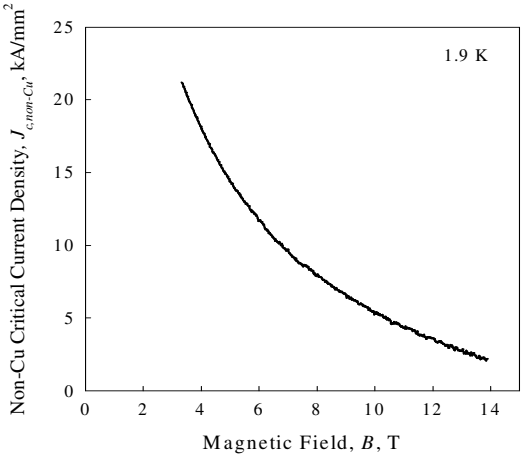

Fig. 3. Magnetically determined $J_{c,non\text{-}Cu}$ versus field strength.

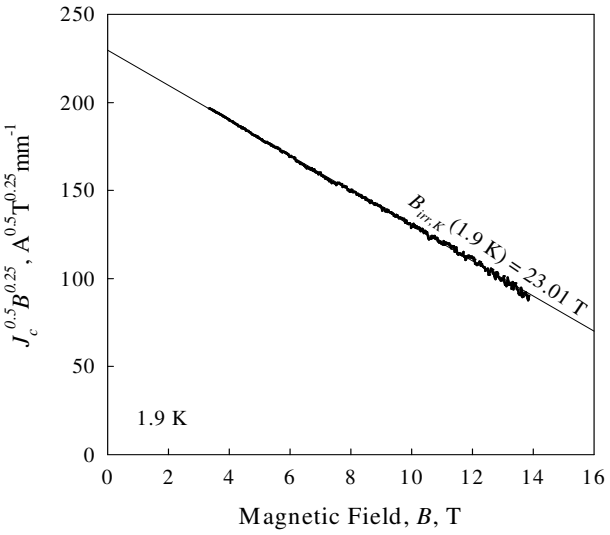

Fig. 4. Kramer plot of $J_{c,non\text{-}Cu}{}^{0.5}$ $B_0{}^{.25}$ versus field strength.

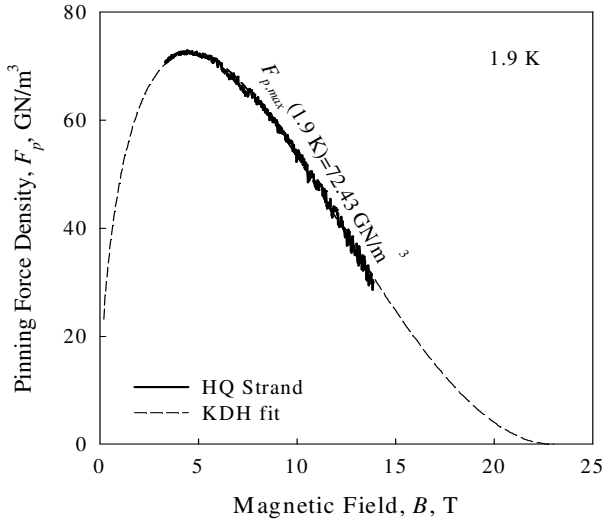

Fig. 5. Bulk pinning force density, F_p, versus field strength. Data fitted to a KDH function for grain boundary pinning at the maximum and given B_{c2} = 23.01 T.

It is worth mentioning at this point that the measurements above were made on a given extracted strand from the cable. As noted above in Table I, the cable contained several different billets (nominally identical), with some level of I_c variation seen by Godeke for extracted strands [22], which in principle would propagate proportionally to magnetization. For this and other reasons, it would be of interest to pursue direct magnetization measurements on cables to allow for second order corrections to the estimates made below.

Under magnet operating conditions supposing that the magnet's load-line meets $J_{c,non\text{-}Cu}(B)$ at 16.5 T the strand's magnetization becomes reduced by a factor $(1\text{-}j^2)$, using a semi-Bean approximation, and where $j = J/J_c$, due to the presence of the transport current [25]. Finally the magnetization of the cable is obtained by taking into account the winding fill factor, in this case 85.5%. The combined results are presented in Table II.

TABLE II SHIELDING MAGNETIZATION OF CABLE HQ1021ZB*

		1	12	14	15	16	16.5
$M_{sh,strand}$	kA/m	200	21.2	13.2	10.0	7.43	
$J_{c,non\text{-}Cu}$	kA/mm^2	48.5	3.55	2.13	1.62	1.26	1.04
$J_{non\text{-}Cu}$	kA/mm^2	0.06	0.76	0.89	0.95	1.01	1.04
$M_{sh,cable}$	kA/m	171	17.2	9.32	5.8	2.03	

* $M_{sh,strand}$ is directly measured below 14 T, KDH-extrapolated above that. $J_{c,non\text{-}Cu}$ is deduced from ΔM and KDH-extrapolated. $J_{non\text{-}Cu}$ is magnet current density along a load line that touches $J_{c,non\text{-}Cu}$ at 16.5 T.

VI. CONCLUSION

As stated above, bench-mark data for the NbTi-wound LHC are $M_{sh,inj,LHC}$ = 10.3 kA/m and $M_{coup,LHC}$ = 2.64 kA/m. The present cable, HQ1021ZB, with an 8 mm stainless steel core wound at LBNL, is similar to a previously measured LBNL-wound HQ-KC3 cable [19]. As such we would expect to find the same 8-mm-core-moderated ICR and coupling magnetization, 1.02 μΩ and 70.3 kA/m, respectively. Clearly such a narrow core width is inadequate to properly suppress M_{coup}.

With regard to persistent-current magnetization at injection, Nb_3Sn's large $J_c d_{eff}$ product guarantees a large value, estimated here to be $M_{sh,cable,inj,1T}$ = 171 kA/m. On the other hand as the magnet is ramped up to operating field $M_{sh,cable}$ steadily decreases such that at 15 T in the windings it has dropped to 5.8 kA/m, clearly an acceptable value.

The M_{coup} results of [19] indicated that a full width core would be needed to adequately suppress coupling magnetization and the $M_{sh,cable}$ data of Table II indicates that although $M_{sh,cable}$ is not a problem close to operating field, strong compensation will be required near injection [26][27].

ACKNOWLEDGMENT

The cables were wound at LBNL by H.C. Higley. Uniaxial compaction was performed at OSU with the assistance of R.J. Baldwin. The cable packs were heat treated at LBNL under the direction of A.K. Ghosh.

REFERENCES

[1] home.web.cern.ch/about/updates/2013/05/birth-higgs-boson
[2] home.web.cern.ch/about/updates/.../long-shutdown-1
[3] L. Bottura, G. de Rijk, L. Rossi, and E. Todesco, "Advanced Accelerator Magnets for Upgrading the LHC", *IEEE Trans. Appl. Supercond.* (2012) 22 4002008 (8 pp.)
[4] M. Karppinen, N. Andreev, G. Apollinari, et al., "Design of 11 T Twin-Aperture Dipole Demonstrator Magnet for LHC Upgrades", *IEEE Trans. Appl. Supercond.* (2012) 22 4901504 (4 pp.); see also M. Karppinen, "11 T Dipole Status May 2012", https://espace.cern.ch/dsdipole/-; see also: hilumilhc.web.cern.ch/hilumilhc/activities/11-T/WP11/
[5] S. Caspi, G. Ambrosio, M. Anerella, E. Barzi, et al., "Design of a 120 mm Bore 15 T Quadrupole for the LHC Upgrade Phase II", *IEEE Trans. Appl. Supercond.* (2010) 20 144-147
[6] V.E.Sytnikov, G.G. Svalov, S.G. Akopov, et al. "Coupling Losses in Superconducting Transposed Conductors Located in Changing Magnetic Fields", *Cryogenics* (1989) 29, 926-930; see also V.E Sytnikov and I.B. Peshkov, "Coupling Losses for Superconducting Cables in Pulsed Fields", *Adv. Cryo. Eng. (Materials)* (1994) 40 537-542
[7] Z. Ang, I. Bejar, L.Bottura, D. Richter, and L.R. Oberli, "Measurement of AC Loss and Magnet Field During Ramps in the LHC Model Dipoles", *IEEE Trans. Appl. Supercond.*(1999) 9 742-745.

[8] A.P Verweij, "Electrodynamics of Superconducting Cables in Accelerator Magnets" Ph.D. Thesis, University of Twente Press, 1995.
[9] T. Boutboul, S. Le Naour, D. Leroy, L. Oberli, and V. Previtali, "Critical Current Density in Superconducting Nb-Ti Strands in the 100 mT to 11 T Applied Field Range", *IEEE Trans. Appl. Supercond.* (2006) 16 1184-1187
[10] Yu. V. Karasev, V. I. Pantsyrny, M. V. Polikarpova, P. A. Lukianov, et al., "$J_c(B,T)$ Characterization of Commercial NbTi Strands for the ITER Poloidal Field Coils by Transport and Magnetization Methods", *IEEE Trans. Appl. Supercond.* (2013) 23 6001304 (4 pp.)
[11] E.W. Collings, M.D. Sumption, M.A. Susner, D.R. Dietderich, E. Kroopshoop, and A. Nijhuis, "Interstrand Contact Resistance and Magnetization of Nb_3Sn Rutherford Cables with Cores of Different Materials and Widths", *IEEE Trans. Appl. Supercond.* (2012) 22 6000904 (4 pp.)
[12] E.W. Collings, M.D. Sumption, M.A. Susner, D.R. Dietderich, E. Kroopshoop, and A. Nijhuis, "Coupling- and Persistent-Current Magnetizations of Nb_3Sn Rutherford Cables with Cores of Stainless Steel and Woven Glass-Fiber Tape Measured by Pick-Up Coil Magnetometry", *IEEE Trans. Appl. Supercond.* (2013) 23 4702305 (5 pp.)
[13] E.W. Collings , M.D. Sumption, M.A. Susner, E. Barzi, D. Turrioni, R. Yamada, et al., "Coupling- and Persistent-Current Magnetizations of Nb_3Sn Cables", *IEEE Trans. Appl. Supercond.* (2010) 20 1387-1390
[14] E.W. Collings, M.D. Sumption, D.R. Dietderich, et al., "Influence of Pre-Heat-Treatment Condition on Interstrand Contact Resistance in Nb_3Sn Rutherford Cables by Calorimetric AC-Loss Measurement", *Adv. Cryo. Eng. (Materials)* (2006) 52 851-858
[15] M.D. Sumption, E.W. Collings, D.R. Dietderich, et al., "Magnetic Measurements of Interstrand Contact Resistance in Nb_3Sn Rutherford Cables in Response to Variation in Pre-Heat-Treatment Condition", *IEEE Trans. Appl. Supercond.* (2006) 16 1200-1203
[16] M.D. Sumption, R.M. Scanlan, Y. Ilyin, et al., "Magnetic, Calorimetric, and Transport Studies of Coupling and Interstrand Contact Resistance in Nb_3Sn Rutherford Cables with Bimetallic Cores of Stainless Steel Bonded to Copper" *Adv. Cryo. Eng. (Materials)* (2004) 50 781-788
[17] E.W. Collings, M.D. Sumption, G. Ambrosio, Y. Ilyin, A. Nijhuis, "Interstrand Contact Resistance in Nb_3Sn Cables under LARP-Type Preparation Conditions", *IEEE Trans. Appl. Supercond.* (2007) 17 (2) 2494-2497
[18] E. W. Collings, M. D. Sumption, M. A. Susner, D. R. Dietderich, and A. Nijhuis, "Coupling Loss, Interstrand Contact Resistance, and Magnetization of Nb_3Sn Rutherford Cables With Cores of MgO Tape and S-Glass Ribbon", *IEEE Trans. Appl. Supercond.* (2011) 21 2367-2371
[19] E. W. Collings, M.D. Sumption, M. A. Susner, D. R. Dietderich, E. Krooshoop and A. Nijhuis, "Interstrand Contact Resistance and Magnetization of Nb_3Sn Rutherford Cables with Cores of Different Materials and Widths", *IEEE Trans. Appl. Supercond.* (2012) 22 6000904 (4 pp.)
[20] E.W. Collings, M.D. Sumption, M.A. Susner, D.R. Dietderich, E. Barzi, A.V. Zlobin, Y. Ilyin, and A. Nijhuis, "Influence of a Stainless Steel Core on Coupling Loss, Interstrand Contact Resistance, and Magnetization of an Nb_3Sn Rutherford Cable", *IEEE Trans. Appl. Supercond.* (2008) 18 1301-1304
[21] H. Felice, S. Caspi, P. Ferracin, V. Kashikin, et al., "Magnetic and Mechanical Analysis of the HQ Model Quadrupole Designs for LARP", *IEEE Trans. Appl. Supercond.* (2008) 18 281-284
[22] A. Godeke, G. Chlachidze, D.R. Dietderich, A.K. Ghosh, M. Marchevsky, M.G.T Mentink and G.L Sabbi, "A review of conductor performance for the LARP high-gradient quadrupole magnets", Supercond. Sci. Technol. 26 (2013) 095015
[23] M.D. Sumption, X. Peng, E. Lee, X. Wu, and E.W. Collings, "Analysis of Magnetization, AC loss, and d_{eff} for Various Internal-Sn Based Nb_3Sn Multifilamentary Strands With and Without Subelement Splitting", *Cryogenics* (2004) 44 711-725
[24] D. Dew-Hughes, "Flux Pinning Mechanisms in Type-II Superconductors", *Phil. Mag.* (1974) 30 293-305
[25] M.A.R. Le Blanc, "Influence of Transport Current on the Magnetization of a Hard Superconductor", *Phys. Rev. Lett.* 11 149-152 (1963).
[26] V.V. Kashikhin and A.V. Zlobin, "Correction of Coil Magnetization Effect in Nb_3Sn High Field Dipole Magnet using Thin Iron Strips", *Fermilab Technical Report* (1999) TD-99-048; see also "Sensitivity of Field Harmonics in Nb_3Sn Dipole Magnet to the Correction Strip Position", *Fermilab Technical Report* (1999) TD-99-068
[27] V.V. Kashikhin and A.V. Zlobin, "Compensation of Strand Magnetization in Superconducting Rutherford Cable with a Thin Iron Core", *Fermilab Technical Report* (2000) TD-00-011